The Lectin-like Domain of Thrombomodulin Confers Protection from Neutrophil-mediated Tissue Damage by Suppressing Adhesion Molecule Expression via Nuclear Factor κB and Mitogen-activated Protein Kinase Pathways

Edward M. Conway,[1] Marlies Van de Wouwer,[1] Saskia Pollefeyt,[1] Kerstin Jurk,[2] Hugo Van Aken,[2] Astrid De Vriese,[1] Jeffrey I. Weitz,[3] Hartmut Weiler,[4] Peter W. Hellings,[1] Paul Schaeffer,[5] Jean-Marc Herbert,[5] Désiré Collen,[1] and Gregor Theilmeier[2]

[1]*The Center for Transgene Technology and Gene Therapy, Flanders Interuniversity Institute for Biotechnology, University of Leuven, B-3000 Leuven, Belgium*

[2]*Klinik und Poliklinik für Anästhesiologie und Operative Intensivmedizin, University of Muenster, D-48149 Muenster, Germany*

[3]*McMaster University and Hamilton Civic Hospital Research Center, Hamilton L8V-1C3, Canada*

[4]*The Blood Center for Southeastern Wisconsin, Milwaukee, WI 53233*

[5]*Sanofi-Synthelabo, Thrombosis Research Department, 31036 Toulouse, France*

Abstract

Thrombomodulin (TM) is a vascular endothelial cell (EC) receptor that is a cofactor for thrombin-mediated activation of the anticoagulant protein C. The extracellular NH_2-terminal domain of TM has homology to C-type lectins that are involved in immune regulation. Using transgenic mice that lack this structure ($TM^{LeD/LeD}$), we show that the lectin-like domain of TM interferes with polymorphonuclear leukocyte (PMN) adhesion to ECs by intercellular adhesion molecule 1–dependent and –independent pathways through the suppression of extracellular signal–regulated kinase $(ERK)_{1/2}$ activation. $TM^{LeD/LeD}$ mice have reduced survival after endotoxin exposure, accumulate more PMNs in their lungs, and develop larger infarcts after myocardial ischemia/reperfusion. The recombinant lectin-like domain of TM suppresses PMN adhesion to ECs, diminishes cytokine-induced increase in nuclear factor κB and activation of $ERK_{1/2}$, and rescues ECs from serum starvation, findings that may explain why plasma levels of soluble TM are inversely correlated with cardiovascular disease. These data suggest that TM has antiinflammatory properties in addition to its role in coagulation and fibrinolysis.

Key words: inflammation • coagulation • endotoxin • sepsis • protein C

Introduction

Thrombomodulin (TM)* is a widely expressed glycoprotein receptor and cofactor for thrombin's activity in a physiologically important natural anticoagulant system. Formation of the thrombin–TM complex limits thrombin's procoagulant and cellular-activating functions and results in thrombin-mediated catalytic transformation of protein C (PC) into activated PC (APC), which in turn down-regulates thrombin generation by degrading coagulation factors Va and VIIIa. TM is also a cofactor for thrombin-mediated activation of plasma procarboxypeptidase B, which is a fibrinolysis inhibitor. In humans, PC deficiency is associated with a hypercoagulable state. Although APC serves as an anticoagulant, it also has antiinflammatory properties, a finding that may explain why APC infusion reduces mortality in patients with sepsis (1). As the critical cofactor for thrombin-mediated activa-

Address correspondence to Edward M. Conway, Center for Transgene Technology and Gene Therapy, KU Leuven, Gasthuisberg O&N, 9th Floor, Herestraat 49, B-3000 Leuven, Belgium. Phone: +32-16-345780; Fax: +32-16-345990; E-mail: ed.conway@med.kuleuven.ac.be

**Abbreviations used in this paper:* AAR, area at risk; APC, activated protein C; BAL, bronchoalveolar lavage; EC, endothelial cell; EGF, epidermal growth factor; ERK, extracellular signal–regulated kinase; ES, embryonic stem; FPA, fibrinopeptide A; GST, glutathione *S* transferase; hpf, high power fields; HUVEC, human umbilical vein EC; ICAM, intercellular adhesion molecule; LV, left ventricle; MAP, mitogen-activated protein; MPO, myeloperoxidase; neo, neomycin phosphotransferase; PC, protein C; PymT, middle T antigen of murine polyomavirus; TM, thrombomodulin; UTR, untranslated region; VCAM, vascular cell adhesion molecule.

 J. Exp. Med. © The Rockefeller University Press • 0022-1007/2002/09/565/13 $5.00
Volume 196, Number 5, September 2, 2002 565–577
http://www.jem.org/cgi/doi/10.1084/jem.20020077

tion of PC, TM is an important bridge that links coagulation and inflammation.

TM is composed of five structural domains. Extending from a short cytoplasmic tail and transmembrane domain is a serine/threonine–rich region to which a chondroitin sulfate moiety that optimizes anticoagulant function is attached (2). Next is a domain that consists of six epidermal growth factor (EGF)-like repeats, four of which are responsible for the protein's anticoagulant and antifibrinolytic functions (3, 4). The NH_2-terminal domain has two modules. The first, adjacent to the EGF-like domain, is an ~70–amino acid residue hydrophobic region. The second, which is ~155–amino acid residues long, has homology to C-type lectins (5), which in many proteins participate in immune and inflammatory processes (6).

Mutational analyses of TM have been restricted to patients with venous or cardiovascular disease and therefore its direct role in inflammation has not been evaluated. Although single nucleotide polymorphisms of TM have been weakly linked with heart disease, these amino acid changes are not within the structures responsible for PC activation (7). Soluble forms of TM derived from the extracellular domain of TM are found in plasma and urine (8, 9). Clinical studies reveal an inverse correlation between plasma levels of soluble TM and coronary artery disease and atherosclerosis (10). Although it has been proposed that the EGF-like repeats of soluble TM promote the generation of APC, which in turn inhibits atherogenesis, it is possible that other components of soluble TM have independent vasculo-protective and antiinflammatory functions.

To evaluate whether the NH_2-terminal domain endows TM with properties distinct from its established role in coagulation and fibrinolysis, we generated mice lacking this structure. We report that the lectin-like domain of TM provides the vascular endothelium with natural antiinflammatory properties by interfering with PMN adhesion. Mice lacking the C-type lectin-like domain have an augmented response to systemic endotoxemia, proinflammatory stimuli in the lung, and myocardial ischemia/reperfusion (MI/R). The lectin-like domain, either soluble or as an intact transmembrane glycoprotein, suppresses intracellular mitogen-activated protein (MAP) kinase pathways, thereby dampening the inflammatory response. Soluble lectin-like domain further protects vascular endothelial cells (ECs) from serum deprivation–induced cell death. The ability of TM to provide natural antiinflammatory protection in concert with its anticoagulant and EC protective properties provides new insights for the development of novel therapies and the elucidation of the etiology of a variety of inflammatory/proliferative disorders.

Materials and Methods

Generation of Mice Lacking the NH_2-terminal Lectin-like Domain of TM via Homologous Recombination in Embryonic Stem (ES) Cells. A 12-kb Kpn1 fragment of the murine *TM* gene containing the coding region was subcloned as previously described (11). The WT coding region was replaced with one that encodes TM lacking the NH_2-terminal domain using PCR-based mutagenesis. Two PCRs were performed. In the first, primer TMs-240 (5′-TTCTGTGGTGGCGCCTGCAGGCCACGCCCG) was paired with antisense primer TMas287i (5′-ATTCTCCACGCTGCA-TAGTGCGGAGAGCCCCAGGCTAGC), resulting in a 541-bp fragment. In the second, sense primer TM.s1957i (5′-GGGC-TCTCCGCACTATGCAGCGTGGAGAATGGTGGCTGT) and TM.as2613EO (5′-TGGACTAGTTAATTAAGATCTTCCTC-GAGGCGCGCCGTTCAGCTGAAATATTTTAGC) yielded a 1,633-bp fragment. The amplicons were used as the target for recombinant PCR with primers TM.s-240 and TM.as2613EO, the latter primer adding Asc1, Xho1, BglII, Pac1, and Spe1 restriction sites. The recombined 2,206-bp amplicon extends from a Nar1 site 230 bp upstream of the transcriptional start site, through the coding region, and 643 bp into the 3′ untranslated region (UTR). The final translated protein product represents intact TM, retaining the first 20 amino acid residues that encompass a putative signal peptide and lacking the subsequent NH_2-terminal 223 amino acid residues of the lectin-like domain (see Fig. 1 A).

A targeting vector to delete the NH_2-terminal domain of TM was constructed (see Fig. 1 A) as previously reported for deletion of the cytoplasmic tail (11), except that *loxP* sites within the 3′-UTR flanked a neomycin phosphotransferase (neo) gene. Not1-linearized targeting vector DNA was introduced into R1 ES cells by electroporation, and homologously recombined colonies were identified by Southern blotting (see Fig. 1 B). The expected deletion was confirmed by PCR of gDNA with primer pair TM.s99 (5′-GTCTAGGTTGTGATAGAGGCT) and TM.as1005 (5′-GGCAGAGGCATCTGGGTTCATT), and DNA sequencing of the 257-bp PCR product.

Targeted ES cells were aggregated and introduced into pseudopregnant female Swiss white mice. Two chimeric male offspring resulted in the germline transmission of the mutant *TM* allele ($TM^{LeDneo/wt}$). F1 and F2 offspring were intercrossed. Genotyping was performed on the tail DNA by Southern blotting and PCR (see Fig. 1 C). Chimeric males were backcrossed with C57Bl/6 and 129sv/ev mouse pedigrees for comparative purposes.

In Vivo Excision of loxP-flanked Neomycin Gene. Mice with a single allele replaced with the mutant TM^{LeDneo} ($TM^{LeDneo/wt}$ mice) were bred with mice homozygous for ubiquitous expression of Cre recombinase under the control of the phosphoglucokinase promoter (12). In vivo excision of the *loxP*-flanked neo from the $TM^{LeDneo/wt}$ mice was confirmed by PCR of gDNA and RT-PCR on RNA from several tissues of offspring (see Fig. 1, D–G). The oligonucleotide primer pair TM.s2520 (5′ GGCTTTGGGTATTTAGTCAGA) and TM.as2700 (antisense 5′ CATAAAACCCAGGCTCACCC) yielded an amplicon of 256 bp when excision was accomplished, whereas the product was 174 bp in length from the WT allele. The resultant $TM^{LeD/wt}$ mice were intercrossed to generate mice with the TM mutation in both alleles. WT siblings from these matings were used as controls ($TM^{wt/wt}$ mice).

Quantitation of TM, Cytokines, and Fibrinopeptide A (FPA). Expression of cell surface TM was confirmed by indirect immunofluorescence (13) using rabbit anti–rat TM antisera (provided by R. Jackman, Brigham and Women's Hospital, Boston, MA), and cofactor activity was evaluated by the activation of PC with thrombin (14). Tissue TM was quantified using a sandwich radioimmunoassay similar to that previously reported (15). ELISA kits (R&D Systems) were used to quantify plasma levels of TNFα,

IL-1β, IL-6, and IL-10. Plasma levels of murine FPA were measured as previously described (11).

Isolation and Growth of ECs. ECs were isolated from murine tumors induced to grow after intraperitoneal injection of retrovirus carrying the middle T antigen of murine polyomavirus (PymT; reference 16). Primary cultures of lymphatic ECs were isolated from intraperitoneal lymphangiomas (17). Experiments were performed with passages three to eight ECs, which were cultured as previously described (13). >95% of the cells stained positive for TM and von Willebrand's factor. Cell survival assays of human umbilical vein ECs (HUVECs) were performed by plating 50,000 cells/well in a 96-well plate in complete media. After 24 h, cells were washed and incubated for 72 h in M199 with 0.05% serum and recombinant protein as indicated. Cell survival was measured with the CellTiter 96 AQ_{ueous} One Solution Cell Proliferation Assay (Promega).

Flow Chamber Experiments. PMNs were isolated from bone marrow (18) and the purity was >95% by Wright staining. Adhesion of PMNs to ECs in a flow chamber was performed as previously described (19). In brief, ECs on collagen-coated glass coverslips were mounted in a parallel flow chamber and superfused with PMN suspensions (2×10^5 cells/ml). Interactions of 2′7′-bis-(2-carboxyethyl)-5-(and 6)-carboxyfluorescein–acetoxymethyl ester (BCECF-AM; Molecular Probes) –labeled PMNs with ECs were observed with an inverted epifluorescence microscope and images were analyzed with NIH Image1.6. Rolling PMNs were counted on five overlays of video frames spanning 50 s of a 5-min experiment. Firm adhesion was determined on 15 high power fields (hpf; 0.9 mm^2/hpf) after rinsing for 5 min. Where noted, ECs were pretreated 4 h before experiments with 200 U/ml recombinant human TNFα (Biosource International).

Static Adhesion Assay. ECs were grown to confluence in 24-well dishes, washed twice with HBSS, and BCECF-AM–labeled PMNs (50,000/well) were added in a final volume of 1 ml for 30 min. Monolayers were washed three times with HBSS and adherent PMNs were counted.

In Vivo Activation of PC. 100 μg human PC (Enzyme Research Labs) was injected intravenously into mice and 15 min later citrated plasma was obtained. Plasma levels of activated human PC were quantified using a capture immunoassay with mAb 7D7B10 (provided by A. Ralston and C. Orthner, American Red Cross, Washington, DC; references 20 and 21). Human PC in murine plasma was measured with the Coamatic PC Assay Kit (Chromogenix) using a standard curve with known quantities of human PC in pooled murine plasma. Each result reflects duplicate measures from at least five mice.

Flow Cytometry Analyses. 3 h after intraperitoneal injection of PBS or 20 μg/g LPS (0111:B4; Sigma-Aldrich), mice were anesthetized and lung vasculature was perfused with PBS. Cell suspensions from lungs (22) were incubated with biotinylated isolectin B1 (*Bandeiraea simplicifolia* I; Sigma-Aldrich) and 5 μg/ml FITC-conjugated rat anti–mouse vascular cell adhesion molecule (VCAM)-1 antibody (CD106) or PE-conjugated hamster anti–mouse intercellular adhesion molecule (ICAM)-1 antibody (CD54; BD Biosciences) at 37°C for 30 min. Suspensions with CD106 or CD54 were additionally incubated with PE-streptavidin or FITC-streptavidin, respectively, followed by final washes with PBS containing 10% FBS. Cell samples were analyzed by flow cytometry using a FACScan™ (Becton Dickinson), gating on isolectin positive ECs. Controls with appropriate irrelevant antibodies excluded nonspecific labeling.

Endotoxin Studies. LPS was injected intraperitoneally into 10–12-wk-old mice. For lethality studies, animals were monitored until the recovery or cessation of breathing. For lung inflammation, 1 mg/ml endotoxin solution was nebulized into mice housing for 10 min. Mice were killed 3 h later by urethane overdose. Blood samples were drawn and the lungs were lavaged five times through a tracheal catheter with 1 ml PBS/5% BSA at 37°C. Bronchoalveolar lavage (BAL) fluid was centrifuged at 4,000 *g* for 5 min. The cell pellet was washed and resuspended in PBS before cell counting and myeloperoxidase (MPO) activity measurements (23). Lungs were dissected and prepared for histological analyses.

MI/R. Myocardial ischemia was induced as previously described (24). In brief, mice were ventilated and body temperature was maintained at 36°C. The left anterior descending coronary artery was ligated over PE-10 tubing. Ischemia of the left ventricle (LV) was maintained for 30 min and then the tubing was removed allowing reperfusion. 3 h later, heparinized saline was infused into the abdominal aorta until no blood was collected from a caval venotomy. The left anterior descending coronary artery was reoccluded and Evans blue was injected into the aortic catheter to delineate the area at risk (AAR). The heart was excised, cut into five slices, each ~1-mm thick, which were immersed in 2% tetrazoliumchloride (25) for the determination of AAR, infarct area, and LV size by planimetry of digitized images.

Generation of Recombinant Protein. Recombinant murine TM, representing the NH_2-terminal 155 amino acids of the mature protein (TM_{lec155}) that was deleted in the $TM^{LeD/LeD}$ mice (starting with AKLQPT...; see Fig. 1) was generated by *Pichia* expression (Invitrogen). Additional purification was accomplished by a series of chromatography steps, including elution of the culture media from a phenyl-Sepharose column, desalting of positive eluates on a G25 column, ion exchange and NaCl gradient elution from a Q-Sepharose column, and size fractionation with superdex-75 in PBS with 0.01% Tween 80. Positive fractions, confirmed by SDS-PAGE and Western blotting with anti-TM antisera, were pooled.

Recombinant TM_{lec155} was also generated as a glutathione *S* transferase (GST) fusion protein (TM_{lec155}-GST) by subcloning the cDNA encoding the first 155 amino acids of TM into the vector pGEX-4T-3 for expression in *Eschericia coli*. Media containing TM_{lec155}-GST was incubated with glutathione-Sepharose, washed, and the TM_{lec155}-GST was eluted from the sepharose beads with excess free glutathione.

Animal Care. Animal experiments were approved by the Institutional Animal Ethics Committee of the University of Leuven, Leuven, Belgium.

Statistical Analyses. Statistical analyses were conducted with the computer programs StatView (Abacus Concepts Inc.) or InStat 2.03 (GraphPad Software). Means are provided with SD unless otherwise noted. P-values were determined using the unpaired *t* test and groupwise comparisons by Wilcox-ranked sum testing.

Results

Mice Lacking the NH_2-terminal Domain of TM Are Viable. Germline transmission of the mutant *TM* allele (Fig. 1) lacking DNA encoding the NH_2-terminal domain was established. Crossbreeding of F1 $TM^{LeDneo/wt}$ mice resulted in >250 offspring (26.1% $TM^{wt/wt}$, 48.7% $TM^{LeDneo/wt}$, and 25.2% $TM^{LeDneo/LeDneo}$), indicating that intrauterine death was not occurring. The neo gene in the 3′-UTR of the mutant allele in $TM^{LeDneo/wt}$ mice was excised in vivo.

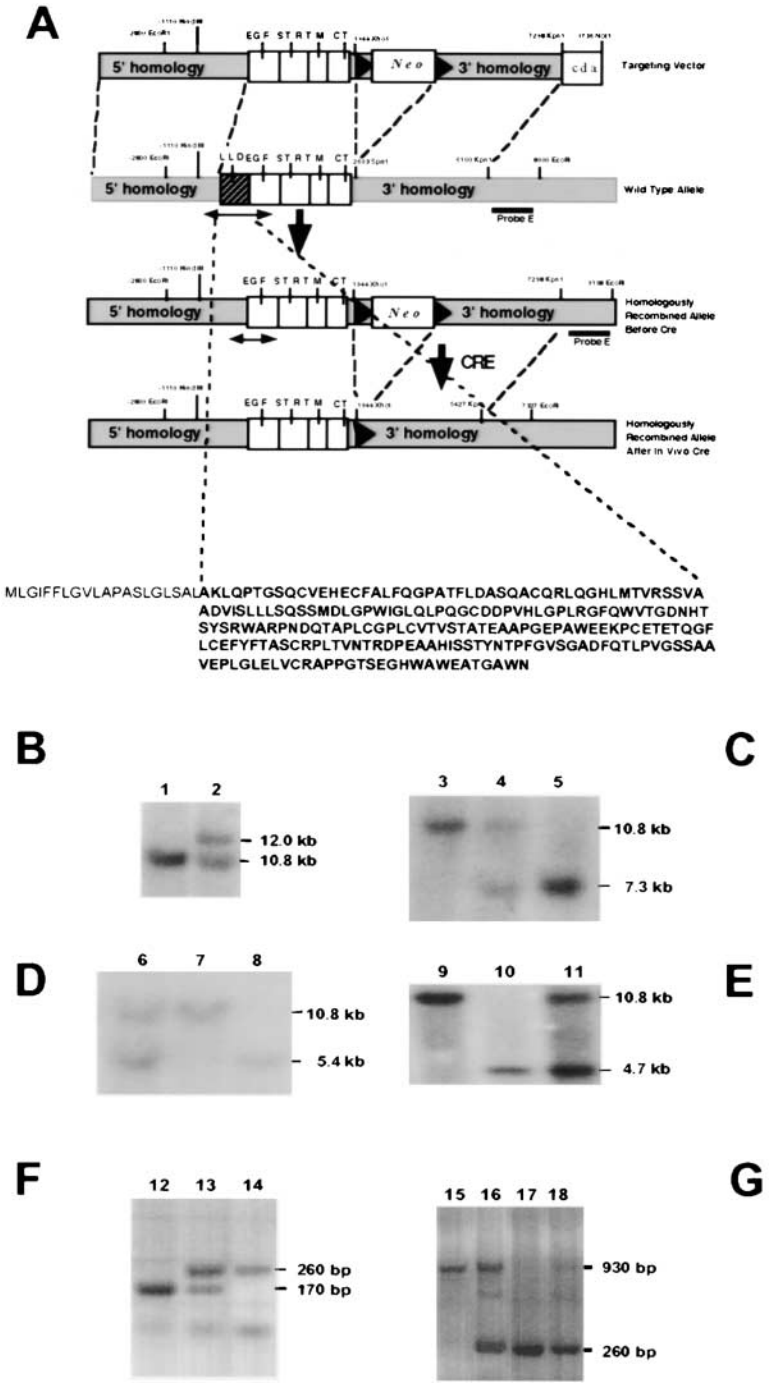

Figure 1. Generation of mice lacking the lectin-like domain of TM. (A) Strategy to introduce TM lacking the NH_2-terminal lectin-like domain into ES cells and mice via homologous recombination. The WT allele for the *TM* gene encodes a lectin-like domain (LLD), six EGF-like repeats (EGF), a serine-threonine rich region (STR), a transmembrane domain (TM), and a cytoplasmic tail (CT). The amino acid sequence of the NH_2-terminal domain that was deleted is shown. (B) Southern blot of EcoR1-digested ES cell gDNA from WT and homologously recombined cells (lanes 1 and 2, respectively) detected with the 3′-external Probe E. The targeted allele is represented with a 12-kb fragment. (C) Southern blot of EcoR1/Xho1-digested tail gDNA from $TM^{wt/wt}$, $TM^{LeDneo/wt}$, and $TM^{LeDneo/LeDneo}$ mice (lanes 3, 4, and 5) detected with Probe E. WT and targeted alleles are represented by 10.8- and 7.3-kb bands, respectively. (D) Southern blot of EcoR1/Xho1-digested tail gDNA from $TM^{LeD/wt}$, $TM^{wt/wt}$, and $TM^{LeD/LeD}$ mice (lanes 6, 7, and 8) using Probe E. (E) Southern blot of EcoR1/Xho1-digested tail gDNA from $TM^{wt/wt}$, $TM^{LeD/LeD}$, and $TM^{LeD/wt}$ mice (lanes 9, 10, and 11) using a HindII/Pme1 internal probe within the 5′-UTR. The WT and targeted alleles are represented by 10.8- and 4.7-kb bands, respectively. (F) PCR confirmation of Cre excision of *neomycin* gene. Primers s2520 and as2700 were used with tail gDNA from $TM^{LeDneo/wt}$, $TM^{LeD/wt}$, and $TM^{LeD/LeD}$ mice (lanes 12, 13, and 14). The WT allele is seen as an ~170-bp amplicon, whereas Cre excision yields an ~260-bp fragment. Amplification did not occur across the intact *neomycin* gene, explaining a single band in lane 12. (G) PCR confirmation of the deletion of the lectin-like domain. Primers s99 and as1005 resulted in an ~930-bp amplicon from the WT allele, and ~260 bp from the targeted allele. Gel shows PCR results using tail gDNA from $TM^{wt/wt}$, $TM^{LeDneo/wt}$, $TM^{LeDneo/LeDneo}$, and $TM^{LeD/LeD}$ mice (lanes 15, 16, 17, and 18).

The resultant $TM^{LeD/wt}$ mice were intercrossed and the genotypes of F2 progeny were also distributed in the expected pattern. Adult $TM^{LeD/LeD}$ and $TM^{wt/wt}$ mice had similar lung TM antigen levels of 360 ± 51 cpm/μg and 370 ± 42 cpm/μg, respectively, whereas levels in the lungs of $TM^{LeDneo/LeDneo}$ mice were ~20% (74 ± 18 cpm/μg) of those in $TM^{wt/wt}$ and $TM^{LeD/LeD}$ mice. All F2 progeny appeared healthy with no differences in weight, growth, or fertility. Backcrossing onto 129sv/se and C57/Bl6 backgrounds resulted in similar phenotypes as reported herein for the Swiss:129sv/se strain.

$TM^{LeD/LeD}$ Mice Have Increased Mortality and Heightened Cytokine Response to Endotoxin. Baseline plasma levels of TNFα, IL-1β, IL-6, and IL-10 were undetectable in all mice and circulating leukocyte counts were normal. 40 μg/g intraperitoneal LPS resulted in the death of >50% of $TM^{LeD/LeD}$ mice within 26 h, whereas <10% of $TM^{wt/wt}$ mice died during the same period (Fig. 2 A). After the addition of 20 μg/g intraperitoneal LPS, TNFα and IL-1β levels at 6 h were significantly higher in mice lacking the NH_2-terminal domain ($P < 0.05$, $n = 18$; Fig. 2 B). Peripheral leukocyte and PMN counts were not significantly

A

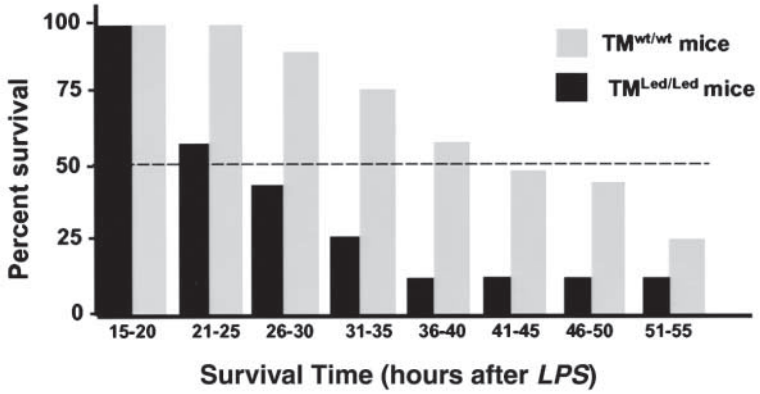

B

Mice	TNFα (ng/ml)	IL-1β (ng/ml)	IL-10 (ng/ml)	WBC (x10³/μl)
TM^wt/wt + *LPS*	63 ± 21	87 ± 32	110 ± 68	0.6 ± 0.4
TM^LeD/LeD + *LPS*	255 ± 91	213 ± 68	138 ± 42	1.2 ± 0.5
TM^LeDneo/LeDneo + *LPS*	318 ± 85	404 ± 116	116 ± 40	0.9 ± 0.4

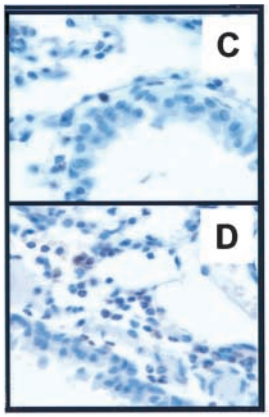

Figure 2. Response of TM$^{LeD/LeD}$ mice to endotoxin. (A) TM$^{LeD/LeD}$ mice and TM$^{wt/wt}$ sibling controls received 40 ug/gm intraperitoneal LPS and survival time was measured. For each group, $n = 22$. (B) 6 h after 20 ug/g intraperitoneal LPS, serum cytokine levels and peripheral leukocyte counts (WBC) were measured. TNFα and IL-1β levels are significantly higher in TM$^{LeD/LeD}$ and TM$^{LeDneo/LeDneo}$ mice. For each group, $n = 18$. (C) Sections of lungs from untreated TM$^{wt/wt}$ and (D) TM$^{LeD/LeD}$ mice were immunostained with MPO for monocytes/PMNs. Positively stained cells, >95% PMNs, are readily detectable in the representative area from the TM$^{LeD/LeD}$ mice.

different ($P > 0.1$). The additional defect of lower TM antigen levels in the TM$^{LeDneo/LeDneo}$ mice did not further affect the cytokine response as compared with TM$^{LeD/LeD}$ mice. Thus, the lack of the NH_2-terminal domain of TM is the sole cause of increased cytokine levels and reduced survival in response to systemic endotoxemia.

Leukocyte Extravasation into Lungs Is Increased in Mice Lacking the NH_2-terminal Lectin-like Domain of TM. Several in vivo models were used to elucidate the function of the lectin-like domain of TM in response to different inflammatory stimuli. In histological sections of the lungs, before intervention, the accumulation of leukocytes (95% PMNs, 5% monocytes) was notably increased in TM$^{LeD/LeD}$ and TM$^{LeDneo/LeDneo}$ mice (Fig. 2, C and D) and distributed throughout the interstitium in peribronchial locations, but rarely in alveolar spaces. No differences were detected when comparing TM$^{LeD/LeD}$ to TM$^{LeDneo/LeDneo}$ mice, indicating that the mechanism is due to the lack of the lectin-like domain rather than the diminished anticoagulant/antifibrinolytic function.

As a trigger for leukocyte-induced lung injury, we exposed mice to inhaled LPS. Baseline MPO activities in BAL fluid were not significantly different between TM$^{wt/wt}$ and TM$^{LeD/LeD}$ mice (87 ± 17 and 92 ± 23 absorbance units, respectively; $n = 4$), consistent with our observation that most PMNs were restricted to the lung interstitium. After LPS inhalation, BAL MPO activity was 3.5-fold higher in the TM$^{LeD/LeD}$ mice than in the TM$^{wt/wt}$ mice (420 ± 31 and 120 ± 50 absorbance units, respectively; $P < 0.005$, $n = 8$), whereas absolute PMN counts were twofold higher. Ultrastructural examination of the LPS-exposed lungs showed mild interstitial PMN accumulation beyond the vessels in peribronchial sites and within the alveoli. Therefore, the lack of the lectin-like domain of TM results in enhanced PMN accumulation in the lungs, an effect that is exacerbated by local exposure to low levels of endotoxin.

TM$^{LeD/LeD}$ Mice Have Larger Infarcts after MI/R. PMN extravasation and cytokine release are hallmarks of MI/R injury (26). In a murine model, the LV area and AAR (11.0 ± 0.9 mm^2 and 10.6 ± 0.7 mm^2, respectively; $P > 0.1$) were similar in TM$^{LeD/LeD}$ and TM$^{wt/wt}$ mice. However, infarct sizes were significantly larger in TM$^{Led/Led}$ than in TM$^{wt/wt}$ mice (Fig. 3, A and B), both as a function of LV size and AAR ($P < 0.002$). To correlate myocardial injury with PMN accumulation, we injected labeled PMNs upon reperfusion, counted adherent PMNs in sectioned hearts, and compared results in corresponding regions of the hearts from TM$^{Led/Led}$ and TM$^{wt/wt}$ mice (Fig. 3, C and D). An average of 22 ± 5 PMNs were found in the AAR of TM$^{wt/wt}$ mice. In the TM$^{Led/Led}$ mice, 2.5 ± 0.7-fold more and 4.8 ± 0.9-fold more PMNs were found in the right and LV, respectively, compared with TM$^{wt/wt}$ mice, indicating that the extravasation of PMNs after MI/R is significantly en-

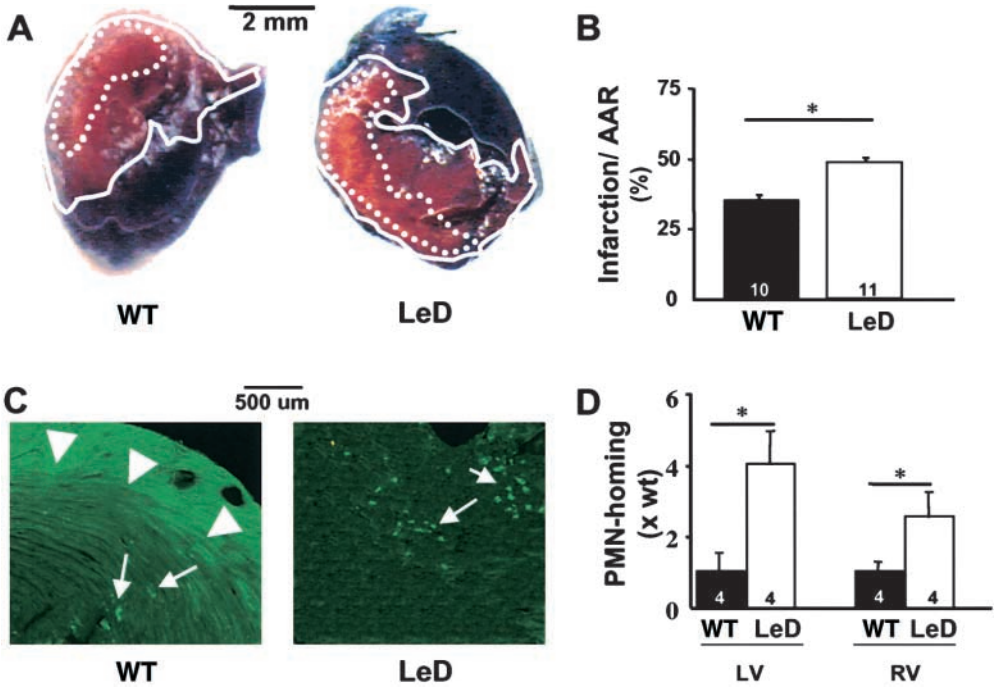

Figure 3. MI/R. (A) In representative MI/R experiments, infarct size relative to AAR, delineated by the dashed and solid lines, respectively, is larger in hearts from $TM^{LeD/LeD}$ mice (LeD) as compared with those from $TM^{wt/wt}$ mice (wt). (B) Infarct size, after MI/R, as a function of AAR is larger in hearts from $TM^{LeD/LeD}$ mice. (C and D) Labeled PMNs were injected upon reperfusion during MI/R, and PMN homing to each ventricle was quantified. (C) Representative sections with more PMNs (arrows) homing to the hearts of $TM^{LeD/LeD}$ mice. Arrowheads show the limit of the AAR, delineated by thioflavin fluorescence. (D) Fold increase, relative to that observed with $TM^{wt/wt}$ mice, of adherent PMNs to the LV and right ventricle (RV) of hearts from $TM^{wt/wt}$ and $TM^{LeD/LeD}$ mice. *, $P < 0.05$.

hanced in the $TM^{LeD/LeD}$ mice ($P < 0.05$, $n = 4$ for each) within and outside the ischemic regions.

Activation of PC by ECs Is Normal in $TM^{LeD/LeD}$ Mice. The preceding results support the conclusion that the NH_2-terminal domain has a specific role in inflammation, which in response to various proinflammatory stimuli, impacts on several organ systems. To definitively exclude the possibility that these findings reflect reduced functional expression of TM in $TM^{LeD/LeD}$ mice with consequent diminished activation of PC, independent methods were used to evaluate APC generation.

We first confirmed that the capacity to activate PC was intact in $TM^{LeD/LeD}$ mice by determining that the administration of human PC did not result in significant differences in plasma concentrations of APC in $TM^{wt/wt}$ and $TM^{LeD/LeD}$ mice ($P > 0.5$; Fig. 4 A). Although the addition of 20 μg/g intraperitoneal LPS 2 h before administering the PC yielded higher levels of APC, there was no difference between the responses of $TM^{wt/wt}$ and $TM^{LeD/LeD}$ mice. We then determined in vitro that the accumulation of TM mRNA and cell surface thrombin-dependent activation of PC by ECs derived from $TM^{LeD/LeD}$ and $TM^{wt/wt}$ mice ($TM^{LeD/LeD}$ ECs and $TM^{wt/wt}$ ECs, respectively) were similar for both cultured lymphatic ECs and PymT-transformed endothelioma cells (Fig. 4, B and C).

Although the data verify that PC activation is intact in the $TM^{LeD/LeD}$ mice, we sought additional confirmation in response to stresses. Predicting that a deficiency in APC would be revealed by a hypercoagulable state, we exposed mice to hypoxia (5.5% oxygen for 18 h; reference 11) to provoke fibrin deposition. Baseline levels of lung tissue fibrin (21) were similar in $TM^{wt/wt}$ and $TM^{LeD/LeD}$ mice (25 ± 17 and 36 ± 25 μg/g, respectively; $P > 0.1$, $n = 10$/group), as were plasma levels of FPA (3.2 ± 2.1 and 4.6 ± 2.5 nM, respectively; $P > 0.1$). Hypoxia did not affect either of these measures. During hypoxia, one $TM^{LeD/LeD}$ mouse and one $TM^{wt/wt}$ mouse died, whereas 7 of 18 $TM^{LeDneo/LeDneo}$ mice died with diffuse lung fibrin deposition, thus substantiating the model. To extend these observations, a second model was used to induce a hypercoagulable state. 20 μg/g intraperitoneal LPS induces fibrin deposition in the lungs of TM-deficient mice with diminished PC cofactor activity (27). After this dose of LPS, fibrin deposits in sectioned lungs, brain, and kidney were similar in the $TM^{LeD/LeD}$ and $TM^{wt/wt}$ mice and quantitative levels of lung tissue fibrin were not increased from the baseline in the $TM^{wt/wt}$ or $TM^{LeD/LeD}$ (unpublished data).

The results indicate that APC generation is not diminished in the $TM^{LeD/LeD}$ mice, supporting the conclusion that the NH_2-terminal lectin-like domain of TM plays a direct role in interfering with the recruitment of inflammatory cells.

Conversion of PMN Rolling to Firm Adhesion Is More Efficient on $TM^{LeD/LeD}$ ECs. We evaluated the mechanisms responsible for excess accumulation of PMNs in the tissues of $TM^{LeD/LeD}$ mice. Because PMNs and monocytes also synthesize TM (28, 29), increased leukocyte efflux could reflect altered TM expression on inflammatory cells/endothelium. To explore these possibilities, we first evaluated the trafficking of PMNs from $TM^{wt/wt}$ and $TM^{LeD/LeD}$ mice across fEND.5 cells, a PymT-transformed murine EC line that expresses TM. At a laminar shear rate of $120s^{-1}$ in a parallel plate flow chamber, the firm adhesion of PMNs from $TM^{wt/wt}$ and $TM^{LeD/LeD}$ mice to unperturbed fEND.5 cells was 62 ± 6 (SEM) and 63 ± 8 (SEM) cells per 15 hpf, respectively ($n = 5$ experiments). After TNFα activation of

A

Mice	hPC (μg/ml)	hAPC (ng/ml)	hAPC after *LPS* (ng/ml)
$TM^{wt/wt}$	8.6 ± 1.3	7.8 ± 2.0	14.0 ± 0.4
$TM^{LeD/LeD}$	9.2 ± 1.8	5.4 ± 1.8	12.9 ± 5.1

B

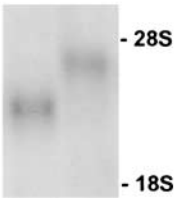

C

Murine Source of Endothelial Cells	ΔOD_{405}/min/10^6 cells	
	Lymphatic Endothelial cells ($n=3$)	Endothelioma Endothelial cells ($n=3$)
$TM^{wt/wt}$	0.24 ± 0.04	0.36 ± 0.05
$TM^{LeD/LeD}$	0.26 ± 0.03	0.34 ± 0.06

Figure 4. Activation of PC is normal in the absence of lectin domain of TM. (A) Plasma levels of human PC (hPC) and human APC (hAPC) after infusion of hPC as described in Materials and Methods. The results reflect one of two representative experiments with five mice in each group. (B) Northern analysis of 20 μg total lymphatic EC RNA from $TM^{LeD/LeD}$ (LeD) or $TM^{wt/wt}$ (wt) mice, detected with a TM cDNA probe. (C) ECs from $TM^{wt/wt}$ or $TM^{LeD/LeD}$ mice were cultured and cell surface thrombin–dependent activation of PC was measured. Results are representative of studies on three clones.

the fEND.5 cells, the number of rolling $TM^{wt/wt}$ and $TM^{LeD/LeD}$ PMNs and their rolling distances were similar, whereas the speed of $TM^{LeD/LeD}$ PMNs was marginally reduced by ~20% (similar results on $TM^{wt/wt}$ ECs; $P = 0.03$). With TNFα activation of fEND.5 cells, the adhesion of $TM^{wt/wt}$ and $TM^{LeD/LeD}$ PMNs was similarly increased 1.6–2-fold. Therefore, TM expression by $TM^{LeD/LeD}$ PMNs does not appreciably contribute to the augmented PMN extravasation observed in vivo in the $TM^{LeD/LeD}$ mice.

To examine the effect of endothelial TM on PMN trafficking, we used PymT-transformed ECs from $TM^{wt/wt}$ and $TM^{LeD/LeD}$ mice. Three different clones of ECs of each genotype yielded similar results. Again, the source of the PMNs had no significant effect on rolling/adhesion parameters. Under resting conditions, 11.1 ± 6 ($n = 6$) PMNs rolled on $TM^{wt/wt}$ ECs, resulting in a permanent adhesion of 36 ± 9 PMNs (Fig. 5 A). Although the number of rolling PMNs on resting $TM^{LeD/LeD}$ ECs was not significantly different, the permanent adhesion of PMNs to the $TM^{LeD/LeD}$ ECs was 7.8-fold greater than to the $TM^{wt/wt}$ ECs. Rolling PMNs traveled 49 ± 5 μm on $TM^{wt/wt}$ ECs with an average speed of 0.7 ± 0.06 μm/sec ($n = 82$) before adhering or returning to the stream. In contrast, the distance traveled by PMNs on $TM^{LeD/LeD}$ ECs was 30% less, and the PMN rolling speed was 55% less than that seen with $TM^{wt/wt}$ ECs ($P < 0.0001$, $n = 286$), indicating that the conversion of PMNs from rolling to firm adhesion is more efficient on $TM^{LeD/LeD}$ ECs.

Next, we studied the effects of the activation of ECs on PMN rolling/adhesion. Stimulation of $TM^{wt/wt}$ ECs with TNFα resulted in a 6.8-fold increase in firmly adhering PMNs as compared with resting $TM^{wt/wt}$ ECs (Fig. 5 A). Furthermore, the distance traveled by PMNs was reduced by 56%, and their speed by 58% ($P < 0.0001$, $n = 41$), evidence that TNFα enhances the conversion of PMN rolling to firm adhesion. This effect was more pronounced when $TM^{LeD/LeD}$ ECs were activated. PMN adhesion was increased an additional 3.1-fold over that observed with activated $TM^{wt/wt}$ ECs.

Similar increases in PMN adhesion to $TM^{LeD/LeD}$ ECs were observed under static conditions (Fig. 5 A). Anti-TM antisera, directed against regions within and outside the NH_2-terminal domain, increased PMN adhesion to $TM^{wt/wt}$ ECs ($P < 0.005$) to levels not different from those seen with $TM^{LeD/LeD}$ ECs ($P > 0.05$). However, the adhesion of PMNs to $TM^{LeD/LeD}$ ECs was unaffected by anti-TM antisera.

PMN Adhesion to $TM^{LeD/LeD}$ ECs Is ICAM-1–dependent and –independent. To identify adhesion molecules mediating enhanced PMN extravasation in $TM^{LeD/LeD}$ mice, we first determined by flow cytometry that suspensions of ECs from lungs of $TM^{LeD/LeD}$ mice expressed more ICAM-1 (median fluorescence 20.2 vs. 4.8) and VCAM-1 (median fluorescence 2.1 vs. 1.6) than ECs from lungs of $TM^{wt/wt}$ mice (Fig. 6 A). Furthermore, the proportion of ECs from the lungs of $TM^{wt/wt}$ and $TM^{LeD/Led}$ mice staining positive for ICAM-1 was 68% and 98%, respectively, whereas for VCAM-1 it was 38% and 51%, respectively. Western blotting of heart lysates also showed greater expression of these adhesion molecules in $TM^{LeD/LeD}$ mice before and after LPS (Fig. 6 B). In view of the central role that ICAM-1 plays in PMN–EC interactions, we characterized the extent of its involvement in PMN adhesion to the $TM^{LeD/LeD}$ ECs in dynamic studies (Fig. 5 B). ICAM-1 blocking did not affect PMN rolling on either $TM^{LeD/LeD}$ or $TM^{wt/wt}$ ECs in the presence or absence of TNFα, nor did it alter adhesion to resting $TM^{wt/wt}$ ECs. After TNFα activation of $TM^{wt/wt}$ ECs, saturating amounts of anti–ICAM-1 antibodies (25 μg/ml) blocked 72 ± 12% ($n = 5$) of PMN adhesion. In contrast, anti–ICAM-1 antibodies only reduced PMN adhesion to resting $TM^{LeD/LeD}$ ECs by 42 ± 4% ($n = 4$) and not to the level of adhesion seen with resting $TM^{wt/wt}$ ECs.

A

Treatment of Endothelial Cells	Dynamic PMN Adhesion (no. per 15 HPFs)		Static PMN Adhesion (no. per 15 HPFs)	
	$TM^{wt/wt}$ Endothelial Cells	$TM^{LeD/LeD}$ Endothelial Cells	$TM^{wt/wt}$ Endothelial Cells	$TM^{LeD/LeD}$ Endothelial Cells
none	36 ± 9	283 ± 66	8 ± 3	63 ± 6
TNF	246 ± 62	767 ± 48	149 ± 6	160 ± 13
Anti-TM antisera			42 ± 2	70 ± 3
Preimmune antisera			9 ± 2	

B

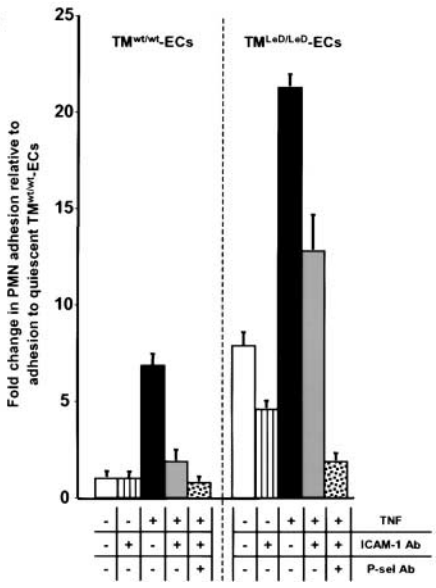

Figure 5. PMN adhesion to $TM^{LeD/LeD}$ and $TM^{wt/wt}$ ECs. (A) Adhesion of PMNs from $TM^{wt/wt}$ or $TM^{LeD/LeD}$ mice to ECs in flow chamber (dynamic) or static adhesion models was measured. Results reflect the mean of at least three independent experiments performed a minimum of three times on three different clones. PMN adhesion was significantly greater to non-TNF–treated $TM^{LeD/LeD}$ ECs than to $TM^{wt/wt}$ ECs ($P < 0.005$). Anti-TM antisera increased PMN adhesion in $TM^{wt/wt}$ ECs ($P < 0.005$), but had no effect on PMN adhesion to $TM^{LeD/LeD}$ ECs. (B) PMNs were assessed for adhesion to $TM^{wt/wt}$ or $TM^{LeD/LeD}$ ECs in a flow chamber in the presence or absence of TNFα and blocking anti–ICAM-1 and/or anti–P-selectin antibodies, as described in Materials and Methods and Results. PMN adhesion to ECs is represented as a fold increase over that observed with quiescent $TM^{wt/wt}$ ECs.

Anti–ICAM-1 antibodies also only partially blocked PMN adhesion by 40 ± 8% ($n = 7$) to TNFα-stimulated $TM^{LeD/LeD}$ ECs. Indeed, suppression was not to the level of adhesion seen with activated $TM^{wt/wt}$ ECs. Although these studies suggest that ICAM-1–independent adhesion is partly responsible for the increased PMN adhesion to $TM^{LeD/LeD}$ ECs, they also indicate that expression levels of ICAM-1 are significantly higher in $TM^{LeD/LeD}$ ECs than in $TM^{wt/wt}$ ECs under the same conditions ($P < 0.03$). Blocking both P-selectin and ICAM-1 suppressed PMN adhesion by >90% and rolling by 65% to TNFα-treated ECs from either $TM^{LeD/LeD}$ or $TM^{wt/wt}$ mice, which is evidence that the predominant defect in $TM^{LeD/LeD}$ EC–PMN interactions occurs after initial contact and rolling. Recent studies have implicated VCAM-1 in mediating PMN emigration in some models of inflammation (30). Consistent with these observations, in preliminary studies maximal doses of anti–VCAM-1 antibodies (25 μg/ml) suppressed TNF-induced PMN adhesion to $TM^{LeD/LeD}$ ECs by ~40%. Overall, the results indicate that receptors involved in PMN rolling are intact in $TM^{LeD/LeD}$ ECs and both ICAM-1 and VCAM-1 enhance PMN adhesion to the $TM^{LeD/LeD}$ ECs, but additional ICAM-1– and VCAM-1–independent pathways are also active in converting PMN rolling to firm adhesion.

Activation of Extracellular Signal–regulated Kinase (ERK)$_{1/2}$ Is Modulated by the NH_2-terminal Domain of TM. The MAP kinase intracellular signaling pathway is implicated in regulating the expression of adhesion molecules (31). We examined the activation of $ERK_{1/2}$ in heart lysates of mice before and after LPS exposure. Total $ERK_{1/2}$ levels remained stable (Fig. 6 C). In mice treated with PBS, baseline levels of phosphorylated $ERK_{1/2}$ were similar between genotypes. After LPS, heart lysates from $TM^{wt/wt}$ mice exhibited little phosphorylation of $ERK_{1/2}$. In contrast, a significant increase in the activation of $ERK_{1/2}$ was detected in heart lysates of $TM^{LeD/LeD}$ mice. These data suggest that the lectin-like domain of TM suppresses LPS-induced phosphorylation of $ERK_{1/2}$.

Soluble Lectin-like Domain of TM Suppresses $ERK_{1/2}$ Activation, Interferes with PMN Adhesion to ECs, and Rescues ECs from Serum-deprived Death. To further evaluate the role of TM in PMN adhesion to ECs, we generated soluble recombinant forms of the molecule comprised of the C-type lectin-like structure in *Pichia pastoris* (TM_{lec155}) and a GST-fusion protein (GST–TM_{lec155}). In static assays (Fig. 7 A), TM_{lec155} significantly reduced PMN adhesion to unstimulated $TM^{LeD/LeD}$ ECs to levels observed with unstimulated $TM^{wt/wt}$ ECs, and adhesion to fEND.5 cells to levels below baseline. PMN adhesion to activated $TM^{LeD/LeD}$ ECs or activated fEND.5 cells was suppressed by TM_{lec155} in a dose-dependent manner. However, PMN adhesion to activated fEND.5 cells could be suppressed to the level observed with nonactivated fEND.5 cells, whereas TM_{lec155} suppressed adhesion to activated $TM^{LeD/LeD}$ ECs only to the level observed with activated $TM^{wt/wt}$ ECs (Figs. 5 A and 7 A). Although the extent of suppression varied in the cell lines tested, soluble lectin-like domain uniformly interfered with PMN adhesion to the ECs.

We predicted that soluble lectin-like domain of TM would suppress PMN adhesion by altering the regulation of MAP kinase pathways in ECs. Therefore, HUVECs were exposed to 200 U/ml TNFα for 20 min. The accumulation of $pERK_{1/2}$ and NF-κB were markedly suppressed, although not totally abrogated, by the addition of GST-TM_{lec155}, whereas GST alone had no effect (Fig. 7 B). Total $ERK_{1/2}$ levels remained unchanged. TM_{lec155} similarly

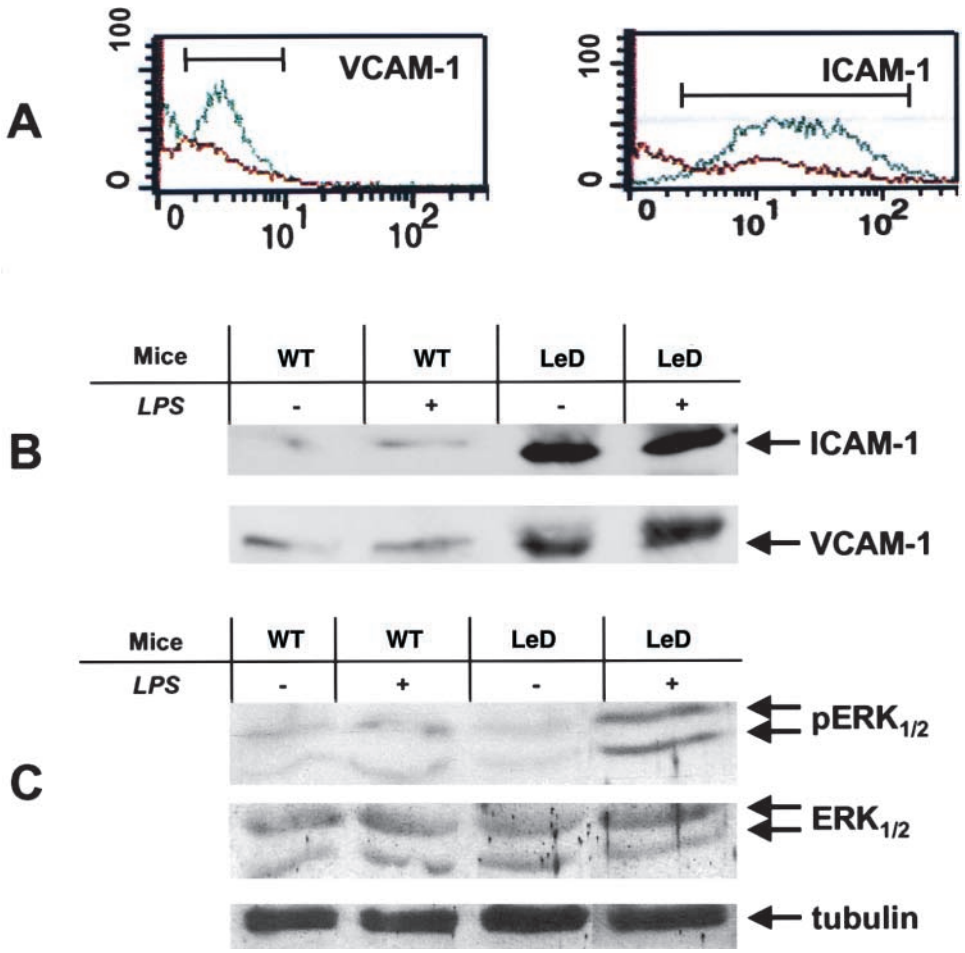

Figure 6. Up-regulation of adhesion molecules in $TM^{LeD/LeD}$ mice. (A) Flow cytometric detection of adhesion molecules. After gating on isolectin positive ECs (20,000 events) of lung suspensions from $TM^{wt/wt}$ (red) and $TM^{LeD/LeD}$ mice (green), surface expression of VCAM-1 and ICAM-1 was detected. In this representative experiment, more adhesion molecule expression is observed for $TM^{LeD/LeD}$ cells. (B) Western immunoblot of heart lysates from $TM^{wt/wt}$ (wt) or $TM^{LeD/LeD}$ (LeD) mice 3 h after treatment with intraperitoneal PBS (−) or 20 ug/g LPS (+). In each lane, 200 μg total protein was added. (C) Western immunoblots of heart lysates of mice treated as in B. Total $ERK_{1/2}$ and tubulin show equal loading of protein. Generation of activated $ERK_{1/2}$ ($pERK_{1/2}$) is increased in LPS-exposed hearts of $TM^{LeD/LeD}$ mice.

interfered with TNFα-induced up-regulation of $pERK_{1/2}$ and NF-κB expression by HUVECs, suggesting that the lectin-like domain of TM suppresses PMN adhesion to ECs via MAP kinase signaling.

Because EC death is a pathway of sustained tissue damage, we evaluated whether TM_{lec155} was capable of rescuing HUVECs from serum starvation–induced cell death. After 3 d of serum deprivation, >95% of HUVECs died. Serum starvation with the addition of TM_{lec155} at concentrations of 1, 10, and 20 μg/ml rescued 2 ± 0.6%, 18 ± 7%, and 34 ± 14% of the cells ($P = 0.69$, $P < 0.05$, and $P < 0.05$, respectively, compared with serum-starved controls), indicating that soluble TM may also have prosurvival properties.

Discussion

Transgenic mice lacking the NH_2-terminal domain of TM ($TM^{LeD/LeD}$ mice) have normal TM antigen levels and retain the capacity to generate APC. Compared with $TM^{wt/wt}$ mice, $TM^{LeD/LeD}$ mice exhibit reduced survival in response to endotoxin, have elevated serum cytokine levels, and respond to local proinflammatory stimuli with augmented PMN adhesion, extravasation, and subsequent tissue damage. Even without exposure to inflammatory stimuli, $TM^{LeD/LeD}$ mice accumulate more PMNs in their lung parenchyma, possibly increasing their risk of tissue damage. These results suggest that the NH_2-terminal lectin-like domain of TM has direct antiinflammatory properties, thereby extending its function to a system beyond coagulation and fibrinolysis.

Although it has long been recognized that the coagulation system modulates inflammation, only recently has the impact of this contribution been appreciated, and some of the molecular links been established. The PC pathway is particularly relevant (32), a fact highlighted by the demonstration that APC infusion reduces mortality in patients with sepsis (1).

As the critical cofactor for PC activation, TM is an obligate participant in the regulation of inflammation. Cytokines and PMN-derived elastase suppress endothelial TM functional and antigenic expression (33, 34), resulting in decreased APC generation, which contributes to the thrombotic and inflammatory components of coronary atheroma (35). Independent of its role in PC activation, we hypothesized that the NH_2-terminal domain of TM might be important in immune defense because of its homology to C-type lectins.

A

Source of Endothelial Cells	Recombinant TM_{lec155}	PMN Adhesion (no. per 15 HPFs)	
$TM^{wt/wt}$		10 ± 6	
$TM^{LeD/LeD}$		39 ± 21	P<0.001
$TM^{LeD/LeD}$	3.6 μg	15 ± 6	P<0.001
$TM^{LeD/LeD}$	7.2 μg	12 ± 7	P=0.017
$TM^{LeD/LeD}$ + TNF		212 ± 53	P<0.001
$TM^{LeD/LeD}$ + TNF	3.6 μg	132 ± 90	P<0.001
$TM^{LeD/LeD}$ + TNF	7.2 μg	153 ± 106	P=0.28
fEND.5		131 ± 82	P=0.008
fEND.5	3.6 μg	103 ± 36	
fEND.5 + TNF		250 ± 58	P<0.001
fEND.5 + TNF	3.6 μg	211 ± 69	P<0.001
fEND.5 + TNF	7.2 μg	153 ± 48	P=0.06

B

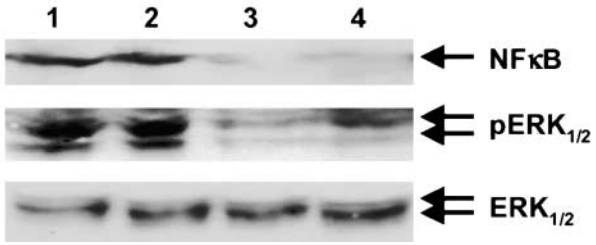

Figure 7. Effects of soluble lectin-like domain of TM on PMN adhesion, NF-κB, and MAP kinase activation. (A) In a static adhesion model, TM_{lec155} significantly decreased PMN adhesion to $TM^{LeD/LeD}$ ECs and fEND.5 cells. (B) Regulation of ERK activation by soluble lectin-like domain of TM. HUVECs were exposed to TNFα (1), TNFα plus GST (2), TNFα plus GST-TM_{lec155} (3), or TNFα plus TM_{lec155} (4) for 20 min. Western immunoblots of cell lysates detected TNFα-induced up-regulation of $pERK_{1/2}$ and NF-κB, which were suppressed by the addition of GST-TM_{lec155} or TM_{lec155}. No change in total $ERK_{1/2}$ was detected. In the absence of TNFα, there was no detectable $pERK_{1/2}$ or NF-κB (not depicted).

The family of C-type lectins has several members including, for example, the selectins (36) and rat AA4 antigen (37). Through interactions with carbohydrate recognition domains, lectins participate in innate immune functions such as opsonization, complement activation, and leukocyte homing (6, 38). Electron microscopic analysis suggests that the lectin-like domain of TM is globular and well-situated for interactions with other proteins or cells (39), as it is located furthest from the membrane surface. The remarkable similarity between AA4 and TM in terms of their structural organization, cellular distribution, and colocalization of their genes to the same chromosomal region (40) suggests a common ancestry and possibly common functions. However, AA4 promotes leukocyte adhesion (40), whereas TM interferes with PMN adhesion. It will be interesting to explore the possibility that TM and AA4 play opposing roles in inflammation and do so via common interacting proteins/intracellular signaling pathways.

To elucidate the mechanism(s) by which the tissues of $TM^{Led/Led}$ mice accumulate more PMNs, we studied leukocyte trafficking and established that even though TM is expressed by PMNs, monocytes, and ECs (28, 29), the critical determinant regulating PMN adhesion is restricted to the NH_2-terminal domain of endothelial TM. Enhanced PMN adhesion to resting $TM^{LeD/LeD}$ ECs suggests that these cells are in a basal proadhesive state, consistent with the findings of excess PMNs in the lungs and increased recruitment of PMNs to nonischemic regions of the hearts of $TM^{LeD/LeD}$ mice. In spite of enhanced firm adhesion to $TM^{LeD/LeD}$ ECs, flow chamber studies indicate that PMN rolling is not affected by lack of the lectin-like domain. Thus, it is possible that the lectin-like domain competes for selectin-mediated outside-in signaling, an event that initiates downstream firm adhesion (41). Consequently, lack of this domain would result in sustained signals and increased expression of proadhesive molecules. ICAM-1, which is higher in the lungs, hearts, and ECs of $TM^{Led/Led}$ mice, clearly contributes to augmented PMN adhesion in $TM^{Led/Led}$ mice. Interestingly, VCAM-1 expression was also augmented in the lungs and hearts of $TM^{LeD/LeD}$ mice. Although VCAM-1 has not traditionally been viewed as a major player in PMN trafficking, recent reports show that $\alpha_4\beta_1$ (VLA-4) integrin and VCAM-1 may contribute to PMN migration in some tissues in response to specific inflammatory stimuli (30, 42), notably including MI/R. As with anti–ICAM-1 antibodies, anti–VCAM-1 antibodies only partially interfered with PMN adhesion to cytokine-stimulated $TM^{LeD/LeD}$ ECs. These data indicate that VCAM-1 and ICAM-1 mediate, in part, the proinflammatory phenotype of the $TM^{LeD/LeD}$ mice, but also suggest that other adhesion molecules, recruited via signals modulated by the lectin-like domain of TM, contribute to this phenomenon. Additional studies are necessary to explore the relative contribution of these and other proadhesive molecules in specific vascular beds under different inflammatory conditions.

Recent in vitro data indicate that APC mediates intracellular signals that down-regulate *NF-κB*, *ICAM-1*, *VCAM-1*, and *E-selectin* gene expression (43). The lectin-like domain of TM may function via similar intracellular pathways. Indeed, the lectin-like domain of TM when constitutively expressed on the cell surface, facilitates intracellular signaling that suppresses PMN adhesion. This interaction may be reversed in response to ischemic or inflammatory stimuli if this domain is cleaved by elastase, or expression of TM is down-regulated (14, 44). Lack of the lectin-like domain of TM in the heart and lungs of $TM^{LeD/LeD}$ mice results in the activation of MAP kinase $ERK_{1/2}$, a signaling pathway that leads to the up-regulation of proinflammatory molecules (31). It is unlikely that the cytoplasmic domain of TM is directly involved in transmitting these signals, because mice lacking this domain do not have an altered cytokine response (unpublished data; reference 11). Alternatively, signaling may occur from the NH_2-terminal domain of TM to other associated cell surface or extracellular soluble proteins, or via its transmembrane domain. Similar examples of cross talk between integrins and other membrane receptors have been documented (45).

Because the tertiary structure of TM is unknown, we cannot exclude the possibility that the NH_2-terminal domain masks a proadhesive domain on TM. A likely candidate region would be the first two EGF-like repeats, these structures being classically involved in protein–protein interactions. These EGF-like repeats could provide a receptor site for activated PMNs that is unmasked during inflammation by allosteric changes in the NH_2-terminal domain or by its cleavage by proteases released from PMNs. Thus, our finding that exogenous soluble TM decreases activation of $ERK_{1/2}$, NF-κB, and PMN adhesion could be explained in part by steric interference with the proadhesive effect of the EGF-like repeats.

Extravasation of activated PMNs during MI/R results in tissue injury that may be attenuated by preventing the expression of cell adhesion molecules such as P-selectin, E-selectin, and ICAM-1 (46). Two polymorphisms of TM, one within the sixth EGF-like repeat (A455V; reference 47) and one within the lectin-like domain (Ala25Thr; reference 48), are associated with increased risk of coronary artery disease/myocardial infarction. The increase in infarct size in the $TM^{Led/Led}$ mice after MI/R supports a direct cardioprotective role for the NH_2-terminal domain, at least in part by interfering with PMN extravasation and cytokine generation. It is intriguing to consider that soluble TM, either the anticoagulant EGF-containing fractions or those fractions that contain the NH_2-terminal domain, might be directly protective, thereby explaining the Atherosclerosis Risk in Communities Study results in which plasma TM levels were inversely correlated with incident coronary heart disease (10). This hypothesis is also supported by a report that soluble human urinary TM, composed of the entire extramembranous portion of TM, prevented hepatic ischemia/reperfusion injury in dogs (49).

Our observation that the lectin-like domain of TM attenuates MAP kinase activation is also interesting in light of clinical data demonstrating an inverse correlation between tumor cell proliferation and TM expression (50). MAP kinase signaling may enhance cellular proliferation by increasing cyclin D1. In tumor models, lack of the NH_2-terminal domain of TM enhances cell growth (51), an effect that may reflect augmented MAP kinase activation. The clinical significance of these findings is highlighted by studies demonstrating that soluble TM has thrombin-independent antitumor effects (52).

Our studies show that the NH_2-terminal lectin-like domain of TM modulates inflammation by attenuating MAP kinase activation and interfering with PMN–EC interactions. We also demonstrate that soluble lectin-like domain enhances cell survival. TM is therefore an example of a highly regulated, multidomain molecule that provides molecular links between several biological systems. Consequently, we predict that mutations in different functional domains of TM produce distinct disease states. Searches have identified TM mutations that are associated with increased thrombotic risk (53, 54), and the Ala25Thr mutation/polymorphism in the lectin-like domain is linked with a higher risk of myocardial infarction (48). Computer modeling indicates that Ala25 is located on an exposed surface of the lectin-like structure. Thus, a mutation at Ala25 could alter the overall hydrophobicity and/or its interaction with other proteins, resulting in a change in function. This finding underlines the importance of considering TM mutations when searching for the etiology of inflammatory/proliferative disorders.

Lastly, the therapeutic potential of these findings cannot be overlooked. Although APC has been shown to provide protection from sepsis, this treatment is not uniformly effective nor is it without a risk of bleeding (1). Studies are underway to determine whether nonanticoagulant forms of soluble TM have therapeutic benefit.

We thank the laboratory personnel at Sanofi-Synthelabo and the Center for Transgene Technology and Gene Therapy for their help, and Bob Jackman and Peter Carmeliet for their input.

G. Theilmeier was supported in part by Innovative Medizinishe Forschung grants TH110023 and IZKF C21.

Submitted: 16 January 2002
Revised: 11 July 2002
Accepted: 26 July 2002

References

1. Bernard, G.R., J.L. Vincent, P.F. Laterre, S.P. LaRosa, J.F. Dhainaut, A. Lopez-Rodriguez, J.S. Steingrub, G.E. Garber, J.D. Helterbrand, E.W. Ely, et al. 2001. Efficacy and safety of recombinant human activated protein C for severe sepsis. *N. Engl. J. Med.* 344:699–709.
2. Nawa, K., K. Sakano, H. Fujiwara, Y. Sato, N. Sugiyama, T. Teruuchi, M. Iwamoto, and Y. Marumoto. 1990. Presence and function of chondroitin-4-sulfate on recombinant human soluble thrombomodulin. *Biochem. Biophys. Res. Commun.* 171:729–737.
3. Kokame, K., X. Zheng, and J. Sadler. 1998. Activation of thrombin-activatable fibrinolysis inhibitor requires epidermal

growth factor-like domain 3 of thrombomodulin and is inhibited competitively by protein C. *J. Biol. Chem.* 273: 12135–12139.
4. Suzuki, K., T. Hayashi, J. Nishioka, Y. Kosaka, M. Zushi, G. Honda, and S. Yamamoto. 1989. A domain composed of epidermal growth factor-like structures of human thrombomodulin is essential for thrombin binding and for protein C activation. *J. Biol. Chem.* 264:4872–4876.
5. Petersen, T. 1988. The amino-terminal domain of thrombomodulin and pancreatic stone protein are homologous with lectins. *FEBS Lett.* 231:51–53.
6. Drickamer, K. 1988. Two distinct classes of carbohydrate-recognition domains in animal lectins. *J. Biol. Chem.* 263: 9557–9560.
7. Ohlin, A.K., and R.A. Marlar. 1999. Thrombomodulin gene defects in families with thromboembolic disease–a report on four families. *Thromb. Haemost.* 81:338–344.
8. Takano, S., S. Kimura, S. Ohdama, and N. Aoki. 1990. Plasma thrombomodulin in health and diseases. *Blood.* 76: 2024–2029.
9. Yamamoto, S., T. Mizoguchi, T. Tamaki, M. Ohkuchi, S. Kimura, and N. Aoki. 1993. Urinary thrombomodulin, its isolation and characterization. *J. Biochem. (Tokyo).* 113:433–440.
10. Salomaa, V., C. Matei, N. Aleksic, L. Sansores-Garcia, A.R. Folsom, H. Juneja, L.E. Chambless, and K.K. Wu. 1999. Soluble thrombomodulin as a predictor of incident coronary heart disease and symptomless carotid artery atherosclerosis in the Atherosclerosis Risk in Communities (ARIC) Study: a case-cohort study. *Lancet.* 353:1729–1734.
11. Conway, E.M., S. Pollefeyt, J. Cornelissen, I. DeBaere, M. Steiner-Mosonyi, J.I. Weitz, H. Weiler-Guettler, P. Carmeliet, and D. Collen. 1999. Structure-function analyses of thrombomodulin by gene-targeting in mice: the cytoplasmic domain is not required for normal fetal development. *Blood.* 93:3442–3450.
12. Lallemand, Y., B. Luria, R. Haffner-Krausz, and P. Lonai. 1998. Maternally expressed PGK-Cre transgene as a tool for early and uniform activation of the Cre site-specific recombinase. *Transgenic Res.* 7:105–112.
13. Conway, E., M. Boffa, B. Nowakowski, and M. Steiner-Mosonyi. 1992. An ultrastructural study of thrombomodulin endocytosis: internalization occurs via clathrin-coated and non-coated pits. *J. Cell. Physiol.* 151:604–612.
14. Conway, E.M., and R.D. Rosenberg. 1988. Tumor necrosis factor suppresses transcription of the thrombomodulin gene in endothelial cells. *Mol. Cell. Biol.* 8:5588–5592.
15. Kennel, S., T. Lankford, B. Hughes, and J. Hotchkiss. 1988. Quantitation of a murine lung endothelial cell protein, P112, with a double monoclonal antibody assay. *Lab. Invest.* 59: 692–701.
16. Wagner, E.F., and W. Risau. 1994. Oncogenes in the study of endothelial cell growth and differentiation. *Semin. Cancer Biol.* 5:137–145.
17. Mancardi, S., G. Stanta, N. Dusetti, M. Gestagno, L. Jussila, M. Zweyer, G. Lunazzi, D. Dumont, K. Alitalo, and S. Burrone. 1999. Lymphatic endothelial tumors induced by intraperitoneal injection of Freund's adjuvant. *Exp. Cell Res.* 246: 368–375.
18. Lowell, C.A., and G. Berton. 1998. Resistance to endotoxic shock and reduced neutrophil migration in mice deficient for the Src-family kinases Hck and Fgr. *Proc. Natl. Acad. Sci. USA.* 95:7580–7584.
19. Theilmeier, G., T. Lenaerts, C. Remacle, D. Collen, J. Vermylen, and M.F. Hoylaerts. 1999. Circulating activated platelets assist THP-1 monocytoid/endothelial cell interaction under shear stress. *Blood.* 94:2725–2734.
20. Orthner, C.L., B. Kolen, and W.N. Drohan. 1993. A sensitive and facile assay for the measurement of activated protein C activity levels in vivo. *Thromb. Haemost.* 69:441–447.
21. Weiler-Guettler, H., P. Christie, D. Beeler, A. Healy, W. Hancock, H. Rayburn, J. Edelberg, and R. Rosenberg. 1998. A targeted point mutation in thrombomodulin generates viable mice with a prethrombotic state. *J. Clin. Invest.* 101:1–9.
22. Marelli-Berg, F.M., E. Peek, E.A. Lidington, H.J. Stauss, and R.I. Lechler. 2000. Isolation of endothelial cells from murine tissue. *J. Immunol. Methods.* 244:205–215.
23. Bradley, P.P., D.A. Priebat, R.D. Christensen, and G. Rothstein. 1982. Measurement of cutaneous inflammation: estimation of neutrophil content with an enzyme marker. *J. Invest. Dermatol.* 78:206–209.
24. Michael, L.H., M.L. Entman, C.J. Hartley, K.A. Youker, J. Zhu, S.R. Hall, H.K. Hawkins, K. Berens, and C.M. Ballantyne. 1995. Myocardial ischemia and reperfusion: a murine model. *Am. J. Physiol.* 269:H2147–H2154.
25. Fishbein, M.C., S. Meerbaum, J. Rit, U. Lando, K. Kanmatsuse, J.C. Mercier, E. Corday, and W. Ganz. 1981. Early phase acute myocardial infarct size quantification: validation of the triphenyl tetrazolium chloride tissue enzyme staining technique. *Am. Heart J.* 101:593–600.
26. Jordan, J.E., Z.Q. Zhao, and J. Vinten-Johansen. 1999. The role of neutrophils in myocardial ischemia-reperfusion injury. *Cardiovasc. Res.* 43:860–878.
27. Weiler, H., V. Lindner, B. Kerlin, B. Isermann, S. Hendrickson, B. Cooley, D. Meh, M. Mosesson, N. Shworak, M. Post, et al. 2001. Characterization of a mouse model for thrombomodulin deficiency. *Arterioscler. Thromb. Vasc. Biol.* 21:1531–1537.
28. Conway, E., B. Nowakowski, and M. Steiner-Mosonyi. 1992. Human neutrophils synthesize thrombomodulin that does not promote thrombin-dependent protein C activation. *Blood.* 80:1254–1263.
29. McCachren, S.S., J. Diggs, J.B. Weinberg, and W.A. Dittman. 1991. Thrombomodulin expression by human blood monocytes and by human synovial tissue lining macrophages. *Blood.* 78:3128–3132.
30. Bowden, R.A., Z.M. Ding, E.M. Donnachie, T.K. Petersen, L.H. Michael, C.M. Ballantyne, and A.R. Burns. 2002. Role of α4 integrin and VCAM-1 in CD18-independent neutrophil migration across mouse cardiac endothelium. *Circ. Res.* 90:562–569.
31. Hubbard, A.K., and R. Rothlein. 2000. Intercellular adhesion molecule-1 (ICAM-1) expression and cell signaling cascades. *Free Radic. Biol. Med.* 28:1379–1386.
32. Esmon, C.T. 2001. Protein C anticoagulant pathway and its role in controlling microvascular thrombosis and inflammation. *Crit. Care Med.* 29:S48–S52.
33. Nawroth, P., and D. Stern. 1986. Modulation of endothelial cell hemostatic properties by tumor necrosis factor. *J. Exp. Med.* 163:740–745.
34. Glaser, C., J. Morser, J. Clarke, E. Blasko, K. McLean, I. Kuhn, R.-J. Chang, J.-H. Lin, L. Vilander, W. Andrews, et al. 1992. Oxidation of a specific methionine in thrombomodulin by activated neutrophil products blocks cofactor activity. *J. Clin. Invest.* 90:2565–2573.

35. Laszik, Z.G., X.J. Zhou, G.L. Ferrell, F.G. Silva, and C.T. Esmon. 2001. Down-regulation of endothelial expression of endothelial cell protein C receptor and thrombomodulin in coronary atherosclerosis. *Am. J. Pathol.* 159:797–802.
36. Galustian, C., A. Lubineau, C. le Narvor, M. Kiso, G. Brown, and T. Feizi. 1999. L-selectin interactions with novel mono- and multisulfated LewisX sequences in comparison with the potent ligand 3′-sulfated Lewisa. *J. Biol. Chem.* 274: 18213–18217.
37. Dean, Y.D., E.P. McGreal, H. Akatsu, and P. Gasque. 2000. Molecular and cellular properties of the rat AA4 antigen, a C-type lectin-like receptor with structural homology to thrombomodulin. *J Biol. Chem.* 275:34382–34392.
38. Vasta, G.R., M. Quesenberry, H. Ahmed, and N. O'Leary. 1999. C-type lectins and galectins mediate innate and adaptive immune functions: their roles in the complement activation pathway. *Dev. Comp. Immunol.* 23:401–420.
39. Weisel, J.W., C. Nagaswami, T.A. Young, and D.R. Light. 1996. The shape of thrombomodulin and interactions with thrombin as determined by electron microscopy. *J. Biol. Chem.* 271:31485–31490.
40. Dean, Y.D., E.P. McGreal, and P. Gasque. 2001. Endothelial cells, megakaryoblasts, platelets and alveolar epithelial cells express abundant levels of the mouse AA4 antigen, a C-type lectin-like receptor involved in homing activities and innate immune host defense. *Eur. J. Immunol.* 31:1370–1381.
41. Crockett-Torabi, E. 1998. Selectins and mechanisms of signal transduction. *J. Leukoc. Biol.* 63:1–14.
42. Burns, J.A., T.B. Issekutz, H. Yagita, and A.C. Issekutz. 2001. The alpha 4 beta 1 (very late antigen (VLA)-4, CD49d/CD29) and alpha 5 beta 1 (VLA-5, CD49e/CD29) integrins mediate beta 2 (CD11/CD18) integrin-independent neutrophil recruitment to endotoxin-induced lung inflammation. *J. Immunol.* 166:4644–4649.
43. Joyce, D.E., L. Gelbert, A. Ciaccia, B. DeHoff, and B.W. Grinnell. 2001. Gene expression profile of antithrombotic protein c defines new mechanisms modulating inflammation and apoptosis. *J. Biol. Chem.* 276:11199–11203.
44. Hirokawa, K., and N. Aoki. 1991. Regulatory mechanisms for thrombomodulin expression in human umbilical vein endothelial cells in vitro. *J. Cell. Physiol.* 147:157–165.
45. Porter, J.C., and N. Hogg. 1998. Integrins take partners: cross-talk between integrins and other membrane receptors. *Trends Cell Biol.* 8:390–396.
46. Jones, S.P., S.D. Trocha, M.B. Strange, D.N. Granger, C.G. Kevil, D.C. Bullard, and D.J. Lefer. 2000. Leukocyte and endothelial cell adhesion molecules in a chronic murine model of myocardial reperfusion injury. *Am. J. Physiol. Heart Circ. Physiol.* 279:H2196–H2201.
47. Wu, K.K., N. Aleksic, C. Ahn, E. Boerwinkle, A.R. Folsom, and H. Juneja. 2001. Thrombomodulin Ala455Val polymorphism and risk of coronary heart disease. *Circulation.* 103: 1386–1389.
48. Doggen, C.J., G. Kunz, F.R. Rosendaal, D.A. Lane, H.L. Vos, P.J. Stubbs, V. Manger Cats, and H. Ireland. 1998. A mutation in the thrombomodulin gene, 127G to A coding for Ala25Thr, and the risk of myocardial infarction in men. *Thromb. Haemost.* 80:743–748.
49. Kaneko, H., N. Joubara, M. Yoshino, K. Yamazaki, A. Mitumaru, Y. Miki, H. Satake, and T. Shiba. 2000. Protective effect of human urinary thrombomodulin on ischemia-reperfusion injury in the canine liver. *Eur. Surg. Res.* 32:87–93.
50. Hamatake, M., T. Ishida, T. Mitsudomi, K. Akazawa, and K. Sugimachi. 1996. Prognostic value and clinicopathological correlation of thrombomodulin in squamous cell carcinoma of the human lung. *Clin. Cancer Res.* 2:763–766.
51. Zhang, Y., H. Weiler-Guettler, J. Chen, O. Wilhelm, Y. Deng, F. Qiu, K. Nakagawa, M. Klevesath, S. Wilhelm, H. Bohrer, et al. 1998. Thrombomodulin modulates growth of tumor cells independent of its anticoagulant activity. *J. Clin. Invest.* 101:1301–1309.
52. Hosaka, Y., T. Higuchi, M. Tsumagari, and H. Ishii. 2000. Inhibition of invasion and experimental metastasis of murine melanoma cells by human soluble thrombomodulin. *Cancer Lett.* 161:231–240.
53. Ireland, H., G. Kunz, K. Kyriakoulis, P.J. Stubbs, and D.A. Lane. 1997. Thrombomodulin gene mutations associated with myocardial infarction. *Circulation.* 96:15–18.
54. Kunz, G., H.A. Ireland, P.J. Stubbs, M. Kahan, G.C. Coulton, and D.A. Lane. 2000. Identification and characterization of a thrombomodulin gene mutation coding for an elongated protein with reduced expression in a kindred with myocardial infarction. *Blood.* 95:569–576.